

Carbon Dioxide Capture for Storage in Deep Geologic Formations – Results from the CO₂ Capture Project

**Capture and Separation of Carbon Dioxide
from Combustion Sources**

Edited by

David C. Thomas

Senior Technical Advisor

Advanced Resources International, Inc.

4603 Clearwater Lane

Naperville, IL, USA

Volume 1



ELSEVIER

2005

Amsterdam – Boston – Heidelberg – London – New York – Oxford
Paris – San Diego – San Francisco – Singapore – Sydney – Tokyo

Elsevier Internet Homepage – <http://www.elsevier.com>

Consult the Elsevier homepage for full catalogue information on all books, major reference works, journals, electronic products and services.

Elsevier Titles of Related Interest

AN END TO GLOBAL WARMING

L.O. Williams

ISBN: 0-08-044045-2, 2002

FUNDAMENTALS AND TECHNOLOGY OF COMBUSTION

F. El-Mahallawy, S. El-Din Habik

ISBN: 0-08-044106-8, 2002

GREENHOUSE GAS CONTROL TECHNOLOGIES: 6TH INTERNATIONAL CONFERENCE

John Gale, Yoichi Kaya

ISBN: 0-08-044276-5, 2003

MITIGATING CLIMATE CHANGE: FLEXIBILITY MECHANISMS

T. Jackson

ISBN: 0-08-044092-4, 2001

Related Journals:

Elsevier publishes a wide-ranging portfolio of high quality research journals, encompassing the energy policy, environmental, and renewable energy fields. A sample journal issue is available online by visiting the Elsevier web site (details at the top of this page). Leading titles include:

Energy Policy

Renewable Energy

Energy Conversion and Management

Biomass & Bioenergy

Environmental Science & Policy

Global and Planetary Change

Atmospheric Environment

Chemosphere – Global Change Science

Fuel, Combustion & Flame

Fuel Processing Technology

All journals are available online via ScienceDirect: www.sciencedirect.com

To Contact the Publisher

Elsevier welcomes enquiries concerning publishing proposals: books, journal special issues, conference proceedings, etc. All formats and media can be considered. Should you have a publishing proposal you wish to discuss, please contact, without obligation, the publisher responsible for Elsevier's Energy program:

Henri van Dorssen

Publisher

Elsevier Ltd

The Boulevard, Langford Lane

Kidlington, Oxford

OX5 1GB, UK

Phone: +44 1865 84 3682

Fax: +44 1865 84 3931

E.mail: h.dorssen@elsevier.com

General enquiries, including placing orders, should be directed to Elsevier's Regional Sales Offices – please access the Elsevier homepage for full contact details (homepage details at the top of this page).

ELSEVIER B.V.
Radarweg 29
P.O. Box 211, 1000 AE Amsterdam
The Netherlands

ELSEVIER Inc.
525 B Street, Suite 1900
San Diego, CA 92101-4495
USA

ELSEVIER Ltd
The Boulevard, Langford Lane
Kidlington, Oxford OX5 1GB
UK

ELSEVIER Ltd
84 Theobalds Road
London WC1X 8RR
UK

© 2005 Elsevier Ltd. All rights reserved.

This work is protected under copyright by Elsevier Ltd, and the following terms and conditions apply to its use:

Photocopying

Single photocopies of single chapters may be made for personal use as allowed by national copyright laws. Permission of the Publisher and payment of a fee is required for all other photocopying, including multiple or systematic copying, copying for advertising or promotional purposes, resale, and all forms of document delivery. Special rates are available for educational institutions that wish to make photocopies for non-profit educational classroom use.

Permissions may be sought directly from Elsevier's Rights Department in Oxford, UK: phone (+44) 1865 843830, fax (+44) 1865 853333, e-mail: permissions@elsevier.com. Requests may also be completed on-line via the Elsevier homepage (<http://www.elsevier.com/locate/permissions>).

In the USA, users may clear permissions and make payments through the Copyright Clearance Center, Inc., 222 Rosewood Drive, Danvers, MA 01923, USA; phone: (+1) (978) 7508400, fax: (+1) (978) 7504744, and in the UK through the Copyright Licensing Agency Rapid Clearance Service (CLARCS), 90 Tottenham Court Road, London W1P 0LP, UK; phone: (+44) 20 7631 5555; fax: (+44) 20 7631 5500. Other countries may have a local reprographic rights agency for payments.

Derivative Works

Tables of contents may be reproduced for internal circulation, but permission of the Publisher is required for external resale or distribution of such material. Permission of the Publisher is required for all other derivative works, including compilations and translations.

Electronic Storage or Usage

Permission of the Publisher is required to store or use electronically any material contained in this work, including any chapter or part of a chapter.

Except as outlined above, no part of this work may be reproduced, stored in a retrieval system or transmitted in any form or by any means, electronic, mechanical, photocopying, recording or otherwise, without prior written permission of the Publisher.

Address permissions requests to: Elsevier's Rights Department, at the fax and e-mail addresses noted above.

Notice

No responsibility is assumed by the Publisher for any injury and/or damage to persons or property as a matter of products liability, negligence or otherwise, or from any use or operation of any methods, products, instructions or ideas contained in the material herein. Because of rapid advances in the medical sciences, in particular, independent verification of diagnoses and drug dosages should be made.

First edition 2005

Library of Congress Cataloging in Publication Data

A catalog record is available from the Library of Congress.

British Library Cataloguing in Publication Data

A catalogue record is available from the British Library.

ISBN: 0-08-044570-5 (2 volume set)

Volume 1: Chapters 8, 9, 13, 14, 16, 17, 18, 24 and 32 were written with support of the U.S. Department of Energy under Contract No. DE-FC26-01NT41145. The Government reserves for itself and others acting on its behalf a royalty-free, non-exclusive, irrevocable, worldwide license for Governmental purposes to publish, distribute, translate, duplicate, exhibit and perform these copyrighted papers. EU co-funded work appears in chapters 19, 20, 21, 22, 23, 33, 34, 35, 36 and 37. Norwegian Research Council (Klimatek) co-funded work appears in chapters 1, 5, 7, 10, 12, 15 and 32.

Volume 2: The Storage Preface, Storage Integrity Preface, Monitoring and Verification Preface, Risk Assessment Preface and Chapters 1, 4, 6, 8, 13, 17, 18, 19, 20, 21, 22, 23, 24, 25, 26, 27, 28, 29, 30, 31, 32, 33 were written with support of the U.S. Department of Energy under Contract No. DE-FC26-01NT41145. The Government reserves for itself and others acting on its behalf a royalty-free, non-exclusive, irrevocable, worldwide license for Governmental purposes to publish, distribute, translate, duplicate, exhibit and perform these copyrighted papers. Norwegian Research Council (Klimatek) co-funded work appears in chapters 9, 15 and 16.

© The paper used in this publication meets the requirements of ANSI/NISO Z39.48-1992 (Permanence of Paper).

Printed in The Netherlands.

Working together to grow
libraries in developing countries

www.elsevier.com | www.bookaid.org | www.sabre.org

ELSEVIER

BOOK AID
International

Sabre Foundation

Chapter 22

GRACE: EXPERIMENTAL EVALUATION OF HYDROGEN PRODUCTION BY MEMBRANE REACTION

Giuseppe Barbieri¹ and Paola Bernardo²

¹Institute for Membrane Technology (ITM-CNR), University of Calabria,
Cubo 17/C, via Pietro Bucci, 87030 Rende CS, Italy

²University of Calabria, Department of Chemical Engineering and Materials,
Cubo 44, via Pietro Bucci, 87030 Rende CS, Italy

ABSTRACT

Water gas shift reaction, widely used for upgrading H₂ containing streams, was analyzed in a membrane reactor (MR) using tubular Pd/Ag, silica and zeolite-A supported Pd membranes supplied by SINTEF (Norway), the University of Twente (The Netherlands) and the University of Zaragoza (Spain), respectively. MR experiments were carried out investigating the effect of temperature (200–338 °C), reaction pressure (up to 550 kPa), partial pressure difference, sweep factor (0–7.5) and space velocity (472–2308 h⁻¹) on CO conversion and identifying rate determining step (kinetics or thermodynamics).

H₂O/CO feed molar ratio was around the stoichiometric value. However, three different streams were fed to the MR: an equimolecular H₂O/CO stream; an “ATR exit + Extra Steam” stream (20% CO, 20% H₂O, 10% CO₂, 50% H₂); and the outlet stream (partially converted) of a traditional reactor (TR) placed before the MR. TR experiments were also performed at a high SV (15,050 h⁻¹). A commercial, Haldor-Topsoe low temperature Cu–Zn oxides-based catalyst (LK821-2) was employed in both MR and TR.

TR equilibrium conversion (TR-EC) was considered as reference because it is the upper limit for typical reactors. This constraint can be overcome by MR as a consequence of H₂ removal by means of a selective membrane.

CO conversion measured in MR experiments, using the SINTEF and Twente University membranes, significantly overcome the thermodynamic limit for TR, depending also on the operating conditions, mainly temperature, pressure and feed composition. In some cases a total conversion was obtained. Also, the use of a TR before the MR allows the TR-EC to be overcome. The conversion showed by the Zaragoza University membranes slightly overcame the TR-EC. Other parameters such as reaction pressure or sweep factor have a positive effect on conversion.

All the membranes were also characterized by means of permeation measurements with a pressure drop (for single gas) and concentration gradient (for gas mixture) methods. The experimental work provided valuable information about the different membrane types and gives useful experimental information on the membrane WGS reactor concept.

INTRODUCTION

Developed countries worked out a planetary energy policy whose objectives are the rational use of energy and environmental safeguarding. These countries have also taken into account the strategic objective of ensuring energy supply by exploiting different energy sources. The energy–environment connection, which has represented a tendency line, is nowadays becoming the prevailing trend. In particular, the reduction of

greenhouse gases (e.g. CO₂ and CH₄) emission is considered in the Kyoto protocol as one of the major challenges in the air pollution context. Kyoto protocol implementation will have a strong impact on energy source and technology exploitation, favoring lower carbon content sources and higher efficiency conversion technologies.

Membrane reactor (MR) thermodynamic equilibrium is different from that of a TR: selective removal of one or more reaction products drives reaction(s) to the right, thus increasing reactant conversion. Product removal happens as far as a difference in the partial pressures of products exists between the two membrane sides. To calculate MR equilibrium conversion, Barbieri et al.[1] showed that the condition of permeating equilibrium, expressed by the equality of the partial pressures on both membrane sides, must be added to the constraints related to reactive equilibrium.

In a chemical reactor (of finite dimension) conversion depends on kinetics and operating variables (e.g. temperature, feed molar ratio, feed flow rate). Temperature and pressure on the permeate side and sweep factor must be considered for evaluating MR conversion. Furthermore, MR conversion depends on the transport mechanism through the membrane of the permeable species (e.g. Sievert's law) and geometric parameters (e.g. membrane area/thickness ratio). Therefore, a more compact design is possible.

The Grangemouth CO₂ capture project (GRACE) concerns the development of new membrane-based systems for CO₂ capture in petrochemical plants, improving new technologies for hydrogen MRs with a better fuel use and reducing, in the meantime, CO₂ production for a given feedstock.

The reaction studied in this work is water gas shift (WGS):



This reaction is exothermic and characterized by no variation in the number of moles. Thus, the CO equilibrium conversion is favored by low temperature and, in a traditional reactor (TR), it does not depend on the reaction pressure. Figure 1 reports the calculated CO equilibrium conversion in a TR and in an MR,

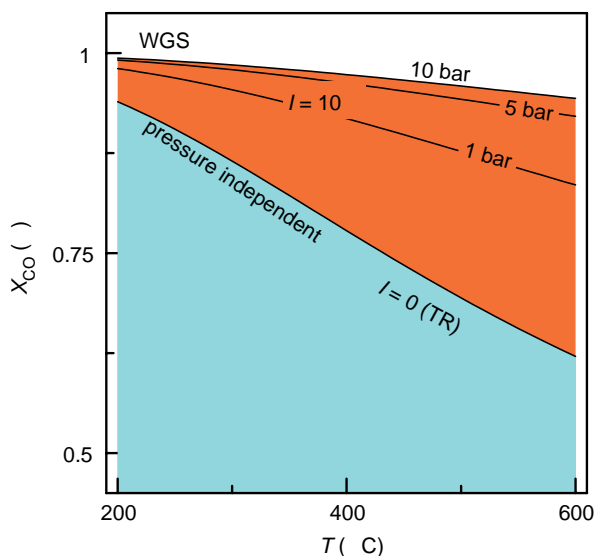


Figure 1: Thermodynamic equilibrium CO conversion vs. T for TR and MR at different reaction pressures [2]. $P^{\text{Permeation}} = 101 \text{ kPa}$, $\text{H}_2\text{O}/\text{CO}$ feed molar ratio (m) = 1, sweep factor (I) = 10.

for different reaction pressures, considering a Pd-based membrane [2]. A higher reaction pressure increases H₂ permeation and thus CO equilibrium conversion in MR is higher than that predicted by thermodynamics for a TR.

Industrially, a Fe–Cr based catalyst at a high temperature (350–420 °C) and a Cu–Zn based catalyst at a medium (250–350 °C) or low temperature (180–250 °C) are employed. A commercial low temperature Cu–Zn oxides based catalyst (Haldor-Topsoe, LK821-2) was used in this work.

In the open literature, some chapters deal with WGS reaction in MRs at an operating temperature higher than 300 °C. Kikuchi et al. [3], working with a Pd-based (glass-supported) MR at 400 °C, reached a complete conversion at a high reaction pressure (500 kPa). Criscuoli et al. [4] measured the CO conversion in a Pd-based MR at 325 °C using three different feed mixtures; complete conversion was achieved with the feed mixture containing less hydrogen (4%) at the lowest SV (highest time-factor ~ 16,000 g_{cat} min CO mol⁻¹). Basile et al. [5] analyzed WGS reaction in MRs, using micro porous ceramic tubes with a thin Pd and Pd/Ag film, in the temperature range 331–350 °C and with a time-factor up to 3000 g_{cat} min CO mol⁻¹ (the same as Ref. [3]), obtaining a maximum conversion of 96.8%.

WGS reaction analysis in MRs investigating the effect of several parameters such as temperature and pressure on both the reaction and permeation sides, trans-membrane pressure difference (ΔP^{TM} , the driving force of permeation), H₂O/CO feed molar ratio (*m*), space velocity (SV), sweep factor (*I*), etc. was carried out.

The operating conditions used are reported in Table 1.

TABLE 1
OPERATING CONDITIONS FOR REACTION IN MRs

Variable	Range
Temperature, °C	210–338
H ₂ O/CO feed molar ratio (<i>m</i>)	~ 1
Space velocity (SV), h ⁻¹	482–2308
Sweep factor (<i>I</i>)	0–7.5
Reaction pressure, kPa	101–550

At a low temperature WGS kinetics is also low. Thus, H₂ partial pressure is too low for a profitable permeation, particularly in the first part of reactor: a higher temperature and/or H₂ containing feed streams were used. Three different configurations were adopted for MR tests (Figure 2). In the first, a mixture of CO and H₂O (*m* ~ 1) was fed to the MR (Figure 2a). Other experiments were carried out with the same molar feed ratio, but using a traditional WGS reactor before the MR (Figure 2b). Therefore, a partially converted stream was fed to MR; due to H₂ presence also in the first part of MR, the membrane was used more profitably. In order to have a more realistic indication of the MR performance in an industrial application, a gas mixture similar to that produced by an oxygen-blown ATR (“ATR + Extra steam”: 20% CO, 20% H₂O, 10% CO₂, 50% H₂) was fed to the MR (Figure 2c).

EXPERIMENTAL

The experimental equipment consists of a furnace, with PID control, containing the MR and the instruments for controlling and monitoring all streams. The furnace available does not allow placing the tubular MR in a vertical position; thus the reactor was placed in a horizontal position. However, when the catalyst was packed in the annular space and in order to avoid by-pass problems, reactants were fed from the bottom and the retentate stream exited from the SS-shell top. An HPLC pump was utilized for liquid water feeding. A coil, located in the furnace, allows water vaporization before its mixing with CO. Mass flow controllers (MFCs, Brooks Instrument 5850S) were used for controlling

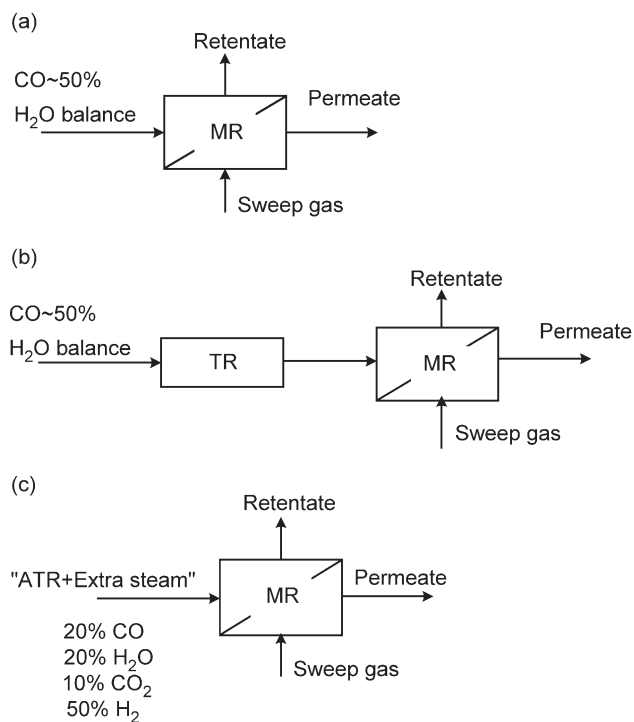


Figure 2: Schemes of the configurations used in reaction tests.

the flow rate of all inlet gaseous streams. Bubble soap flow-meters were used to measure the flow rate of the outlet streams. No automated instrument (e.g. MFC) can be utilized because the outlet composition is not known a priori and is different in each measurement. Back pressure controllers (BPCs, Brooks Instrument 5866) were used to set retentate and permeate pressures at desired values.

Chemical analyses were performed by means of an Agilent 6890N gas chromatograph equipped with two analytical lines: one for the retentate stream and the other for the permeate one. Each line was equipped with two columns: an HP-Plot-5A (for separating permanent gases such as H₂, N₂ and CO) and an HP-Poraplot-Q (for the other species).

The permeation driving force is defined, for each species, as the trans-membrane pressure difference (ΔP_i^{TM}) between the reaction and permeate sides. Any pressure variation generated on outlet streams produces a variation on the species permeation. A GC with one analytical line requires a switching valve that changes the pressures. The GC configuration used in this work allows the analysis of both outlet (retentate and permeate) streams at the same time, avoiding any pressure variation on the reaction and permeation sides, with no effect on the stationary state.

A tube in tube module for tubular membranes and a double cell for flat membranes were used for permeation and reaction tests. A tubular MR is more suitable for an industrial application. On the laboratory-scale, this configuration allows an easier data analysis. It consists of an inner tube, the supported membrane, and an outer one, the SS-shell. The sealing between the SS-shell and the membrane is realized, for each membrane end, by means of a graphite gasket supported by an SS O-ring.

Two tubular MR configurations can be realized when a catalyst is packed: (a) catalyst packed in the core of the tube, (b) catalyst packed in the annular space between the supported membrane and SS-shell. These two configurations are characterized by different conditions, e.g. the overall heat exchange coefficients between the reaction volume and the furnace and those between permeate and reaction streams, etc. [6].

The flat membranes were assembled in an SS-cell by means of teflon O-rings. The membrane separates the two zones, one of which is packed with the catalyst.

MR configuration depends also on the side where the membrane separating layer is located, since a direct contact between the top layer and catalyst pellets can damage the membrane reducing its perm-selectivity properties. Therefore, the catalyst was generally packed on the opposite side with respect to the membrane separating layer, except for third and fourth generation SINTEF membranes covered with an external protective porous layer.

Gas permeation measurements were performed following the pressure drop or concentration gradient methods. In the pressure drop method the permeation driving force (ΔP^{TM}) is the absolute pressure drop applied between the two membrane sides. It was realized setting P^{Feed} and maintaining $P^{Permeate}$ at the atmospheric value (101 kPa). In the concentration gradient method gases are supplied at both membrane sides; in particular, a sweep gas is fed at the permeate side. In this way, permeation is due to concentration gradients: the driving force can be expressed as difference of species partial pressure. This method needs a chemical analysis too.

A permeation test allows measuring the permeating flux through the membrane and evaluating the gas permeance, calculated as the ratio between the permeating flux and ΔP_i^{TM} .

The ratio of the permeance of two gases, measured at the same temperature, is the ideal separation factor (SF). The actual SF is defined, for gas-mixture permeation, using the molar composition of permeate and retentate. The feed fraction that permeates through the membrane is indicated as the *stage-cut* (θ) and it can be also defined for each species.

The main variables considered in reaction tests are temperature, reaction pressure, H₂O/CO feed molar ratio (m) and space velocity. CO conversion of TR was calculated using the equation:

$$\text{CO conversion} = \frac{F_{\text{CO}_2}^{\text{Out}}}{F_{\text{CO}}^{\text{Feed}}}; [-]$$

In an MR, both outlet streams must be taken into account for calculating CO conversion:

$$\text{CO conversion} = \frac{F_{\text{CO}_2}^{\text{Retentate}} + F_{\text{CO}_2}^{\text{Permeate}}}{F_{\text{CO}}^{\text{Feed}}}; [-]$$

The expression used to calculate the CO conversion gives the lowest possible value. In fact, only the CO₂ measured is considered and not the missing CO. The highest value can be obtained adding the “carbon balance”:

$$\text{Carbon balance} = - \frac{F_{\text{CO}}^{\text{Feed}} - (F_{\text{CO}}^{\text{Retentate+Permeate}} + F_{\text{CO}_2}^{\text{Retentate+Permeate}})}{F_{\text{CO}}^{\text{Feed}}}; [-]$$

TR equilibrium conversion (TR-EC), the maximum conversion obtainable in this system, was considered as reference and the conversion measured in MRs was compared with it, even though conversion of a finite TR operating in the same conditions gives a more direct comparison.

Other important variables, characterizing an MR, are P^{Permeate} and the sweep factor (I) which represents the system extractive capacity [6].

For the configuration coupling TR with MR (see Figure 2b) the overall SV was calculated as

$$SV_{\text{TR+MR}} = \frac{Q^{\text{Feed}}}{V_{\text{Catalyst}}^{\text{TR}} + V_{\text{Catalyst}}^{\text{MR}}}; [\text{h}^{-1}]$$

The relationship among SV_{TR} and SV_{MR} and $SV_{\text{TR+MR}}$ is:

$$\frac{1}{SV_{\text{TR+MR}}} = \frac{1}{SV_{\text{TR}}} + \frac{1}{SV_{\text{MR}}}$$

RESULTS AND DISCUSSION

The temperature range considered was 200–338 °C; the reaction pressure was up to 550 kPa and H₂O/CO feed molar ratio (m) was around the stoichiometric value. For the MR, nitrogen, flowing in co-current direction with reactant stream, was used as sweep gas with a sweep factor (I) varying between 0 and 7.5. The space velocity was varied in the range 472–2308 h⁻¹; a value of 2000 h⁻¹ was considered as reference since close to those of industrial interest. In addition, some TR experiments were performed also at 15,050 h⁻¹.

MR Experiments Using SINTEF Pd-based Membranes

Table 2 reports the main characteristics of the Pd-based tubular membranes developed by SINTEF. All membranes have a Pd-based foil covering the central external surface of a tubular SS support; the SS membrane ends are used for connecting together the membrane and MR shell. Therefore, there are two kinds of sealing: one between the Pd-based layer and the support and the other between the membrane and the SS-shell.

The operating procedure indicated by SINTEF was: 300 °C as maximum operating temperature; no exposure to hydrogen at temperature below 200 °C; overpressure from outside to inside because the Pd/Ag layer was a foil covering the support.

The third and fourth generations of SINTEF membranes have a protective filter over the Pd-based layer. Therefore, the catalyst was packed in the annular space of the MR (the same as the membrane side). Consequently, a reaction pressure higher than the permeate pressure was used in this case.

Results of the permeation tests, carried out on SINTEF membranes at different temperatures, with or without sweep gas, are reported in Figure 3. By increasing the temperature a little, a decrease in H₂ permeating flux, and also in the permeance, was observed, while the sweep gas use always resulted in the permeate flux increase.

No N₂ permeation was observed for SINTEF G2-2, indicating the good quality of the membrane. N₂ observed permeation for SINTEF G3-2 is an indication of no ideal membrane behavior or defect presence in the sealing. This is also confirmed by the low ideal SF (H₂/N₂) which is equal to 2.75 at 255 °C and to 2.53 at 286.5 °C. Also, SINTEF G2-3 presented N₂ permeation; however, the ideal SF (H₂/N₂) was 10.3 at 260 °C and 9.3 at 280 °C, higher than measured for SINTEF G3-2. In particular, the H₂ permeating flux is almost equal for the two membranes, while G3-2 has a higher N₂ flux and consequently a reduced ideal SF.

Reaction measurements were performed on SINTEF G1-2 up to 280 °C, varying the SV from 1385 to 2308 h⁻¹ (Figure 4). CO conversion follows the thermodynamic prediction for a SV up to 1847 h⁻¹. At a higher space velocity (2308 h⁻¹) the kinetics becomes the rate determining step.

Also, the reaction experiments performed on SINTEF G2-3 in the temperature range 260–300 °C, at an SV equal to 2085 h⁻¹ are reported in Figure 4. A CO conversion higher than TR-EC was achieved. Thus, better results with respect to SINTEF G1-2 were obtained, even at similar operating conditions, except for

TABLE 2
PD-BASED MEMBRANES SUPPLIED BY SINTEF

Membrane name	Membrane			Support			Characteristics
	OD (mm)	Length (mm)	Average thickness (μm)	Area (cm^2)	Total length (mm)		
SINTEF G1-1	13.35	20	6.75	8.39	70	Porous SS, with drilled 0.5 mm holes	Catalyst packed inside tubular membrane
SINTEF G1-2	13.35	10	1.5	4.19	70	316L SS, Pall AccuSep (pore size of 5 μm)	
SINTEF G2-2	12.70	22	1.95	8.78	78		
SINTEF G2-3	12.70	22	1.13	8.78	78		
SINTEF G3-1	12.70	22	1.3	8.78	78	316L SS, Pall AccuSep (pore size of 5 μm) with a protective filter over the membrane layer	Catalyst packed in the annular space between the membrane and SS-shell
SINTEF G3-2	12.70	22	1.3	8.78	78		
SINTEF G4-1	12.70	22	1.3	8.78	78		

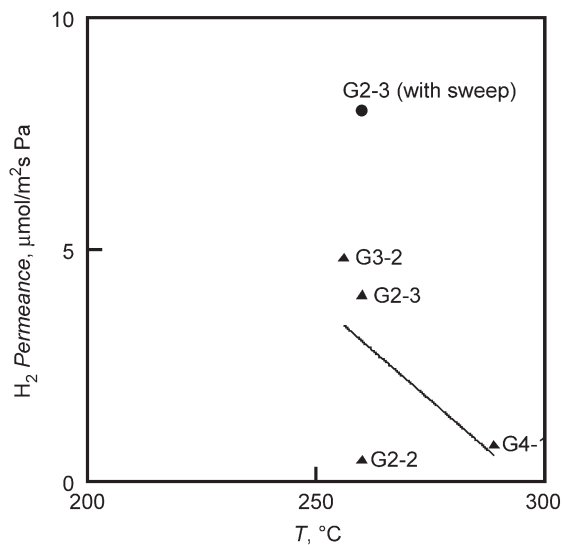


Figure 3: SINTEF Pd-based membranes: H₂ permeance vs. T .

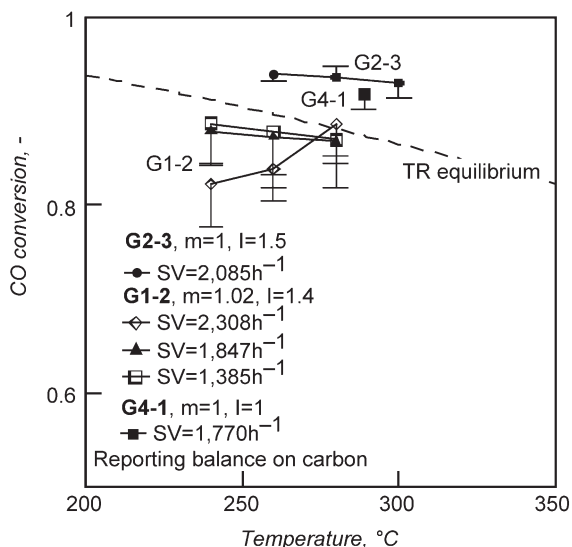


Figure 4: CO conversion vs. T for SINTEF G1-2 ($w_{\text{cat}} = 1.5$ g), SINTEF G2-3 ($w_{\text{cat}} = 4.72$ g) and SINTEF G4-1. Average values (symbols) and mass balance on carbon (connected horizontal dash).

temperature. No significant changes in CO conversion were observed by increasing temperature, even though the difference between the MR and TR-EC increases at higher temperatures.

Reaction tests were also performed on SINTEF G4-1 at 289 °C (Figure 4), working with a sweep factor equal to 1. These first results are very interesting: MR CO conversion (98%) is higher than TR-EC also at a high SV (1770 h^{-1}). In addition to this good conversion value, no N_2 (sweep gas) was found in the retentate stream, while no CO or CO_2 were found in the permeate stream.

Reaction Experiments Coupling TR and MR

Due to the slow WGS kinetics, in the first reactor section the H_2 partial pressure on the reaction side is low; therefore, no significant H_2 permeation can occur. In order to improve CO conversion, a TR was used before the MR as described in Figure 2c; thus, a partially converted stream was fed to the MR. H_2 presence in the stream fed to MR allowed a significant permeation also in the first part of MR, using the Pd-based membrane more profitably.

Experimental results using SINTEF G1-2 (Figure 5), with space velocity values in the range $\text{SV}_{\text{TR+MR}} = 1279\text{--}4138 \text{ h}^{-1}$, were very interesting, since the TR-EC was overcome and the rate determining step was changed from kinetic (only MR) to thermodynamic. In particular, at the lowest temperature a CO conversion increase of 15% (from 82 to 97%) was observed. Less advantage was obtained at the highest temperature.

MR reaction experiments were performed on SINTEF G3-1 at 290 °C (Figure 6): by increasing the sweep factor (up to 2) a higher CO conversion was measured. In order to improve the MR performances, as already done with SINTEF G1-2, a TR was placed before the MR. In this way, a CO conversion higher than TR-EC was measured (Figure 6), particularly at high sweep factor values (up to 8).

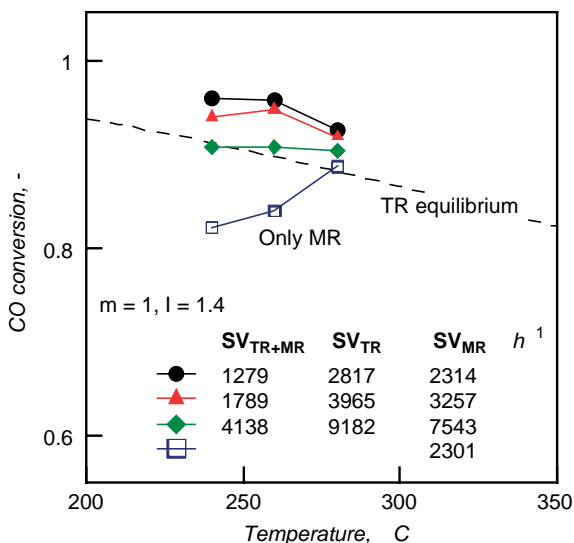


Figure 5: SINTEF G1-2—CO conversion in the (TR + MR) system. $w_{CatTot} = 3.3$ g (1.8 g in the TR and 1.5 g in the MR).

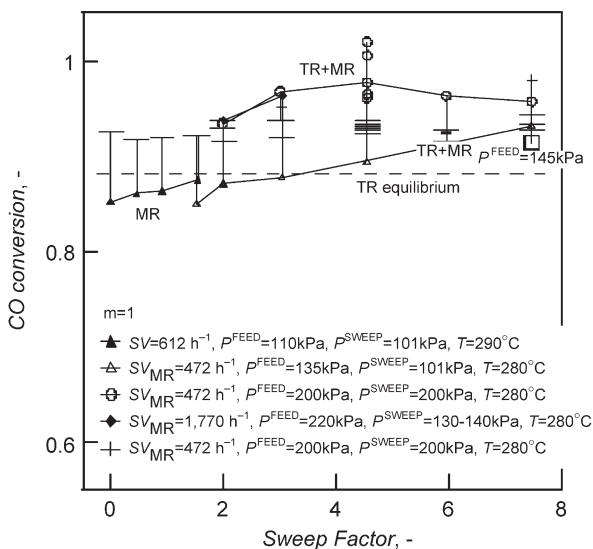


Figure 6: SINTEF G3-1—CO conversion vs. Sweep factor. Average values (symbols) and mass balance on carbon (connected horizontal dash).

A new set of experiments at a low SV_{MR} (472 h^{-1}), but at high P_{Reaction} (200 kPa) showed a high CO conversion (Figure 6). Increasing SV_{MR} (1770 h^{-1}), but with a ΔP^{TM} different from zero (80–90 kPa), very high CO conversions were measured. In this last case, a maximum CO conversion was observed at $I = 4.5$. Other experiments performed at $I = 4.5$, varying the stage-cut, showed a CO conversion almost complete (Figure 6).

Figure 7 reports the same data in terms of stage-cut vs. ΔP^{TM} for H_2 , CH_4 , and CO_2 . Even though the same number of moles of CO_2 and H_2 are formed by the WGS reaction, a higher stage-cut can be observed for H_2 . However, CO presents a low ΔP^{TM} : no CO in the permeate stream and only a little unconverted CO amount in the retentate stream, due to its consumption in the reaction and also to the good quality of the membrane. The distribution of these species suggests the MR works well allowing H_2 permeation and no CO_2 or CO permeation. The small amount of CO_2 in the permeate stream can be due to defects in the sealing between the membrane foil and SS-support.

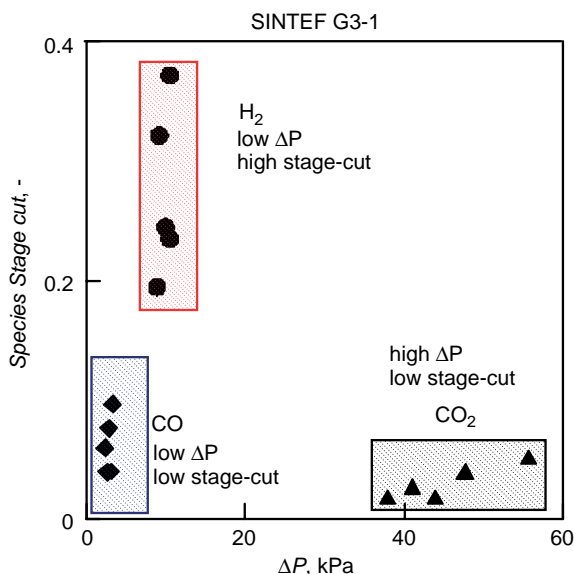


Figure 7: SINTEF G3-1—reaction tests: stage-cut vs. ΔP_i .

Reaction Experiments Using a Feed Stream Close to that of the “ATR Exit + Extra Steam”

MR experiments were performed on SINTEF G2-3 using a feed stream with a composition (20% CO , 20% H_2O , 10% CO_2 and 50% H_2) close to that of the “ATR exit + Extra Steam”. As shown in Figure 8, also in this case, it was possible to achieve CO conversion significantly higher than the TR-EC limit. In the considered temperature range (260–300 °C) CO conversion follows the thermodynamic prediction, thus better conversions were reached working at lower temperatures.

MR Experiments Using Silica Membranes Supplied by Twente University

Table 3 reports a summary of the main characteristics of the membranes supplied by Twente University. These membranes have a silica layer on an inorganic support. Each end has a sealing glaze in order to connect it with the MR shell.

Before any experiment, a pre-treatment procedure indicated by Twente University, was followed: a slow heating at a rate $< 1 \text{ }^\circ\text{C}/\text{min}$ up to 200 °C while permeating H_2 .

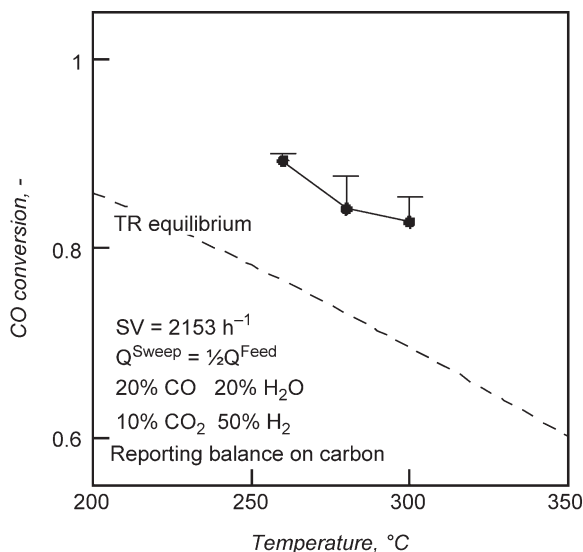


Figure 8: SINTEF G2-3—CO conversion vs. T . Feed stream composition close to that of the “ATR exit + Extra Steam”. Total feed flow rate = $100 \text{ cm}^3(\text{STP})/\text{min}$. Average values (symbols) and mass balance on carbon (connected horizontal dash).

TABLE 3
SILICA MEMBRANES SUPPLIED BY TWENTE UNIVERSITY

Name	Membrane						Support
	Geometry	Separating layer location	OD (mm)	ID (mm)	Length (mm)	Area (cm^2)	Size of each sealed end (mm)
UniTwente 1	Tubular	Internal	10	7	66	14.5	15
UniTwente 2	Tubular	Internal	10	7	90	19.8	5
UniTwente 3	Flat	Upper	39	15.6	—	1.9	7 (annulus)
UniTwente 4	Tubular	Internal	10	7	70	15.4	5
UniTwente 5	Tubular	Internal	10	7	70	15.4	5
UniTwente 6	Flat	Upper	39	15.6	—	1.9	7

In this kind of microporous membranes, the expected transport mechanism is “molecular sieving” with smaller molecules permeating faster through the membrane. Kinetic diameters of the molecules considered in permeation tests are reported in Table 4. Therefore, H_2 is expected to be the most permeable species.

Results of permeation tests with single gases (H_2 , N_2 , CO , CO_2 , CH_4) obtained at different temperatures are reported in Table 5.

During the heating of UniTwente 2 membrane no H_2 permeating flux was observed up to $100 \text{ }^\circ\text{C}$. The so-called “methane test” is a good indicator of the membrane quality since an ideal silica membrane should have zero permeability to CH_4 , due to its high kinetic diameter. At room temperature no methane

TABLE 4
KINETIC DIAMETER OF THE SPECIES USED IN PERMEATION EXPERIMENTS

Species	H ₂ O	H ₂	CO ₂	N ₂	CO	CH ₄
Kinetic diameter, Å	2.65	2.89	3.30	3.64	3.76	3.80

TABLE 5
UNITWENTE MEMBRANES—PERMEATION EXPERIMENTS

Membrane	<i>T</i> , °C	ΔP^{TM} , kPa	Permeance, nmol/m ² s Pa					idealSF- H ₂ /N ₂
			H ₂	CO ₂	N ₂	CO	CH ₄	
UniTwente 1	200	20			470			
	210		1570	392		451	661	3.07
UniTwente 2	188 ^a	290	374				128	
UniTwente 3	186 ^b	300	241.1	15.6	6.1	6.5	Not detected	39.5
	208 ^b		240.7	15.3	5.6	3.7	6.3	43.0
UniTwente 4	157	60	232		4.25		5.21	54.5
	187		299	12.1	4.3		4.6	69.3
	206		365	11.9	4.6		5	79.4
UniTwente 5	250	60	844		143			5.9
		100	895		150			6.0
		160	953		156			6.1

^a CH₄ was not detected at $\Delta P^{TM} = 60$ kPa.

^b N₂, CO, CH₄ were not detected at $\Delta P^{TM} = 60$ kPa.

permeating flux was detected for UniTwente 2 membrane. After the pre-treatment procedure UniTwente 2 membrane presented CH₄ permeability (Table 6).

No H₂ permeating flux was observed up to 100 °C for UniTwente 3 flat membrane. The measured gas permeances were almost independent from ΔP^{TM} and *T*. This latter aspect suggests excluding Knudsen flux as governing the transport mechanism, since Knudsen flux decreases with temperature. The permeation order follows the kinetic diameters: smaller molecules permeate faster. In order to investigate the membrane stability in WGS reaction condition, the UniTwente 3 membrane was exposed to a steam flow for about 7 h. H₂ permeance measured (*T* = 208 °C, $\Delta P^{TM} = 300$ kPa) after steam exposure (97 nmol/m² s Pa), was about 40% that of the precedent value (241 nmol/m² s Pa), suggesting a membrane modification due to water vapor. In fact, the silica layer is hydrophilic and undergoes a structural change in the presence of water vapor. This change consists in a densification of the silica layer with a partial loss of OH groups [7].

Hydrogen permeance for the UniTwente 4 membrane (Table 5) increased with temperature, suggesting an activated transport mechanism. Permeance of other gases, instead, were independent of temperature and almost equal. As a consequence, ideal SF increased with temperature. In addition, experiments were carried out with two feed mixtures of H₂ and N₂:

- Mixture 1, containing 50.38% of H₂
- Mixture 2, containing 77.00% of H₂.

Results of permeation tests with mixtures and pure gases, at *T* = 157 °C and $\Delta P^{TM} = 60$ kPa are reported in Figure 9. Nitrogen presence in the feed stream reduced H₂ permeance of about 95% (Mixture 1) and 70%

(Mixture 2) if compared with pure hydrogen permeance. N_2 permeance, instead, in mixture and as pure gas was approximately the same.

Initially, permeation tests were carried out on Mixture 1 at $T = 157^\circ\text{C}$ and $\Delta P^{\text{TM}} = 60\text{ kPa}$. In these conditions hydrogen permeance was dramatically decreased with respect to pure gas and the stage-cut was about 2.5%. The actual SF (H_2/N_2) values were much lower than the ideal SF.

After the mixture permeation a hydrogen permeation test at $T = 157^\circ\text{C}$ and $\Delta P^{\text{TM}} = 60\text{ kPa}$ was repeated, confirming the permeance of the previous corresponding experiment. Therefore, the membrane was not modified by the mixture permeation; however, slow diffusing nitrogen molecules block the passage to the fast diffusing H_2 molecules.

New permeation tests with Mixture 1 were carried out increasing ΔP^{TM} up to 200 kPa: in this way, the stage-cut was equal to 23.3% and the actual-SF reached the value of 9.5.

Other permeation tests were carried with Mixture 2, richer in hydrogen than Mixture 1. Increasing ΔP^{TM} from 60 up to 200 kPa, the stage-cut varied from 14.3% up to 52.7%, while actual-SF remained almost the same (6.5 and 7.1, respectively).

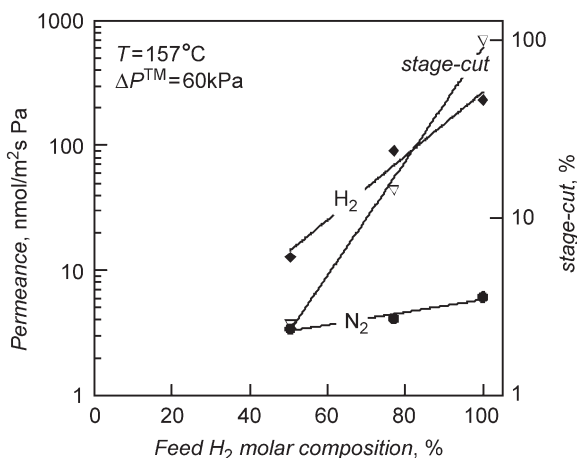


Figure 9: UniTwente 4—permeation measurements with pure gases and mixtures.

The UniTwente 4 membrane was tested, after the mixture permeation, feeding pure H_2 and N_2 and imposing a ΔP^{TM} of 60, 200 and 300 kPa. The permeances measured, particularly for N_2 , resulted almost independent of ΔP^{TM} and only a little reduction in hydrogen permeance ($272\text{ nmol/m}^2\text{ s Pa}$) with respect to the first permeation test ($299\text{ nmol/m}^2\text{ s Pa}$) was observed.

However, another effect that must be taken into account is the seal used for this membrane by the University of Twente that is not completely stable (it cannot be used above 200°C), thus influencing permeation data. As observed by the University of Twente, at a high temperature, volatile constituents from this seal can narrow the membrane pores causing a little permeation decrease with time; the “selectivity is not influenced” by the “seal effect”, while in the present experiments also the ideal SF decreases, since only H_2 and not N_2 permeance decreased.

The UniTwente 5 permeance does not significantly depend on temperature; at 250°C H_2 permeance increased with ΔP^{TM} while that of N_2 was almost constant. H_2 and CH_4 permeance measured at Twente

University on the same membrane were 920 and 2.6 nmol/m² s Pa, respectively, giving an ideal SF (H₂/CH₄) of 354.

H₂ permeance measured for the UniTwente 5 in reaction tests was about the same as measured for pure hydrogen in permeation tests. After reaction tests, other permeation experiments were carried out to investigate the effect of steam exposure. An increase in hydrogen permeance was observed, suggesting pore enlargement. The same effect was found by Giessler et al. [8]. Some permeation tests were repeated on the UniTwente 6 flat silica membrane after the reaction, showing no significant differences (Figure 10, Table 6).

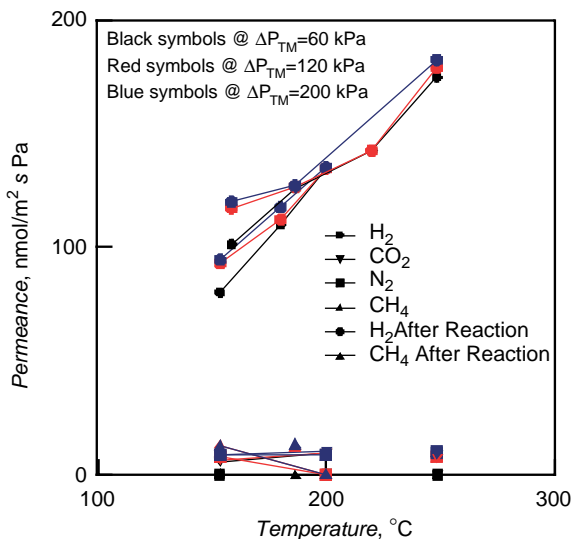


Figure 10: UniTwente 6—permeance vs. T before and after reaction.

TABLE 6
UNITWENTE 6—IDEAL SEPARATION FACTORS BEFORE AND AFTER REACTION

idealSF, -	Before reaction			After reaction		
	ΔP^{TM} , kPa			ΔP^{TM} , kPa		
	60	120	60	60	120	200
	$T = 153\text{ }^{\circ}\text{C}$			$T = 186.5\text{ }^{\circ}\text{C}$		
H ₂ /CO ₂	14.9	14.2	14.2			
H ₂ /N ₂	∞	11.5	∞			
H ₂ /CH ₄	∞	7.2	∞	∞	10.0	-
	$T = 200\text{ }^{\circ}\text{C}$			$T = 248.5\text{ }^{\circ}\text{C}$		
H ₂ /CO ₂	14.3	10.6	13.4	∞	24.7	-
H ₂ /N ₂	∞	11.0	15.8	∞	22.8	-
H ₂ /CH ₄	∞	7.4	∞	∞	16.1	-

MR Experiments Using UniTwente Membranes

MR measurements on the UniTwente 1 membrane were carried out at different temperatures (210–265 °C) and varying space velocity (from 826 to 1776 h⁻¹), maintaining 19.4 g of catalyst. A H₂O/CO feed molar ratio (m) equal to 1 and a sweep factor (l) equal to 1 were the values of the other parameters. The reactants were fed on the annulus side.

An increase in the operating temperature reduces the distance from the TR-EC (Figure 11). In particular, CO conversion was slightly higher than the equilibrium prediction for TR at the lowest SV (828 h⁻¹) and at the highest temperature considered (265 °C).

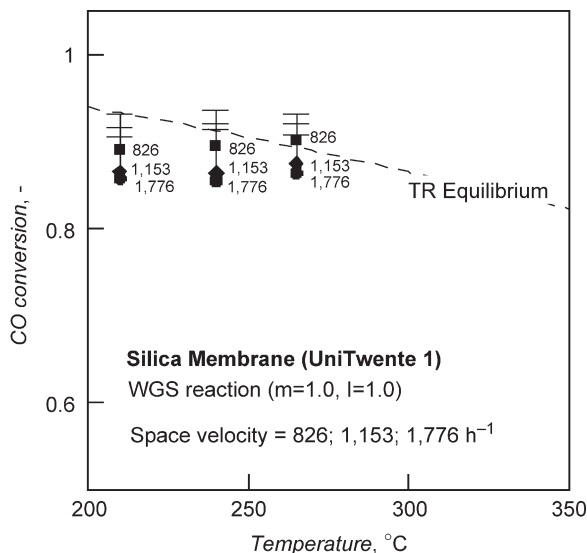


Figure 11: UniTwente 1—CO conversion vs. T .

In order to operate at a higher reaction rate, a temperature up to 320 °C was used (Figure 12). In addition, reaction pressure higher than atmospheric value (up to 550 kPa) was used, thus moving towards industrial specifications. In the temperature range 260–320 °C, CO conversion presents a maximum: kinetics is the rate determining step up to 280 °C, then the behavior follows the thermodynamic equilibrium. For a temperature higher than 250 °C the MR conversion was always higher than the TR-EC limit.

Reaction pressure has a positive effect on MR CO conversion: an increase from 175 to 200 kPa produced a higher conversion for the same sweep factor value (4).

Since the reaction pressure had a positive effect on CO conversion, other reaction experiments were aimed to increase the reaction pressure up to 550 kPa. Figure 13 reports the experimental data obtained for a reaction pressure of 300 kPa. In this case, the higher P_{Reaction} allowed MR CO conversion higher than TR-EC even at a high SV (1823 h⁻¹). A clear positive effect of increasing the sweep factor (0–2) can be also observed.

Higher reaction pressures (500 and 550 kPa) produced a higher CO conversion (Figure 14), above the TR-EC limit, also at $l = 1$. Increasing SV from 1830 to 2017 h⁻¹ no significant CO conversion improvement was observed.

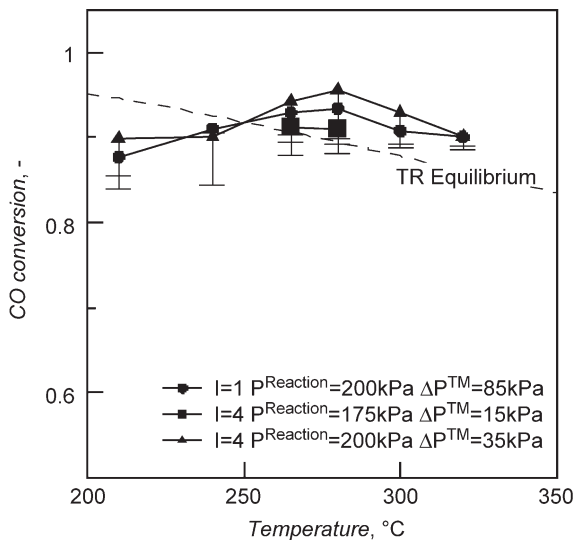


Figure 12: UniTwente 1—CO conversion vs. T . $m = 1.03$, $SV = 826 \text{ h}^{-1}$. Average values (symbols) and mass balance on carbon (connected horizontal dash).

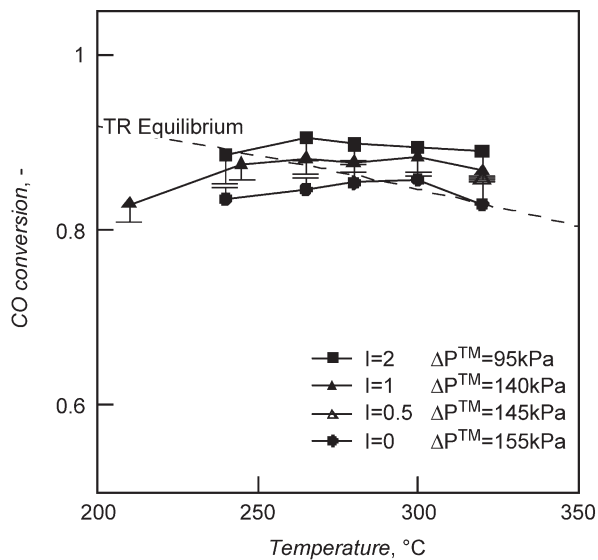


Figure 13: UniTwente 1—CO conversion vs. T . $m = 0.96$, $SV = 1823 \text{ h}^{-1}$, $p_{\text{Reaction}} = 300 \text{ kPa}$. Average values (symbols) and mass balance on carbon (connected horizontal dash).

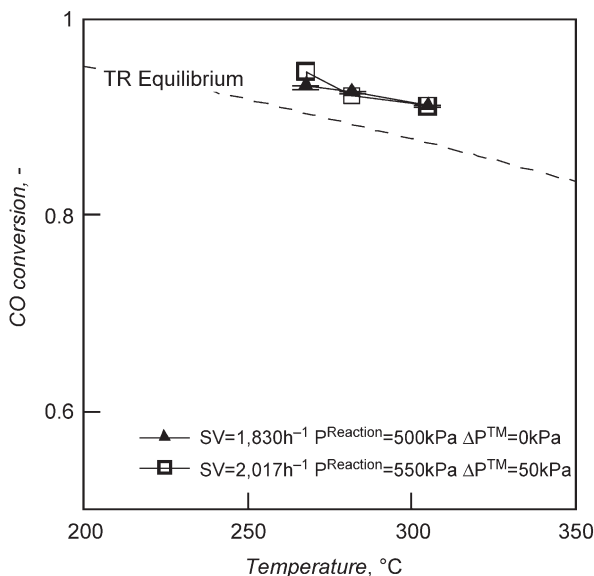


Figure 14: UniTwente 1—CO conversion vs. T . $m = 1.03$, $I = 1.0$.

Reaction tests were carried out on the UniTwente 5 at $T = 300\text{ }^{\circ}\text{C}$, $P^{\text{Reaction}} = 300\text{ kPa}$ and $SV = 1918\text{ h}^{-1}$, varying the sweep factor, which had a negative effect on CO conversion (Figure 15).

Reaction tests were carried out on the UniTwente 6 flat silica membrane at $220\text{ }^{\circ}\text{C}$ and at $250\text{ }^{\circ}\text{C}$ (as suggested by the University of Twente, the operating temperature was lower than $250\text{ }^{\circ}\text{C}$). The experimental data at two different SV values and changing the sweep factor are reported in Figure 16. MR CO conversion at $220\text{ }^{\circ}\text{C}$ was lower than the TR-EC and no significant improvements were found by halving the space velocity (from 1799 to 901 h^{-1}). Increasing the temperature at $250\text{ }^{\circ}\text{C}$ at the lowest space velocity (901 h^{-1}) the TR-EC was overcome.

It is important to note the SV effect: at a lower SV value (901 h^{-1}) there is a thermodynamic control with a CO conversion overcoming TR-EC limit, while at a higher SV value (1799 h^{-1}) kinetics is controlling. However, as already observed for UniTwente 5 membrane, the increase in sweep factor had a negative effect on CO conversion.

MR Experiments Using Pd-based Membranes Supplied by University of Zaragoza

The tubular membranes (ID = 7 mm, OD = 10 mm, length = 60 mm) supplied by Zaragoza University have a Pd film on a zeolite A layer realized on a commercial alumina tube.

In zeolite A microporous membranes smaller molecules permeate faster through the membrane, with an improved H_2 permeance due to the Pd presence.

Permeation Experiments Using UniZaragoza Membranes

Pd-based membranes supplied by the University of Zaragoza were characterized by means of permeation tests with single gases (H_2 , N_2 , CO_2 and CH_4). Table 7 reports the results obtained at different temperatures.

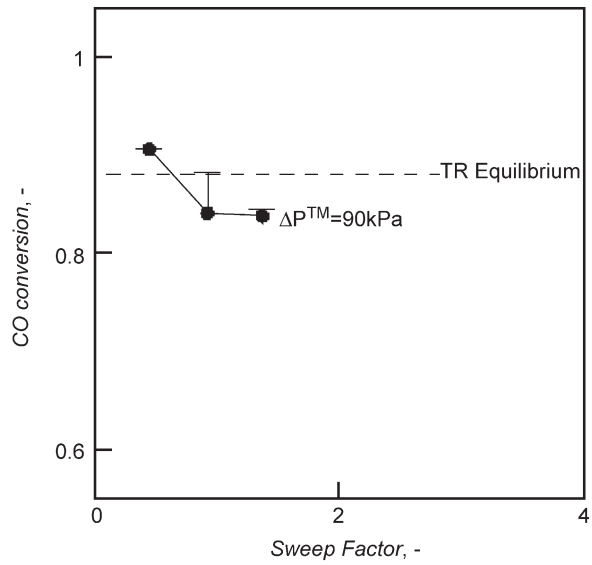


Figure 15: UniTwente 5—CO conversion vs. sweep factor at 300 °C. $m = 1.04$, $SV = 1918 \text{ h}^{-1}$, $p^{\text{Reaction}} = 300 \text{ kPa}$, $\Delta P^{\text{TM}} = 100 \text{ kPa}$. Average values (symbols) and mass balance on carbon (connected horizontal dash).

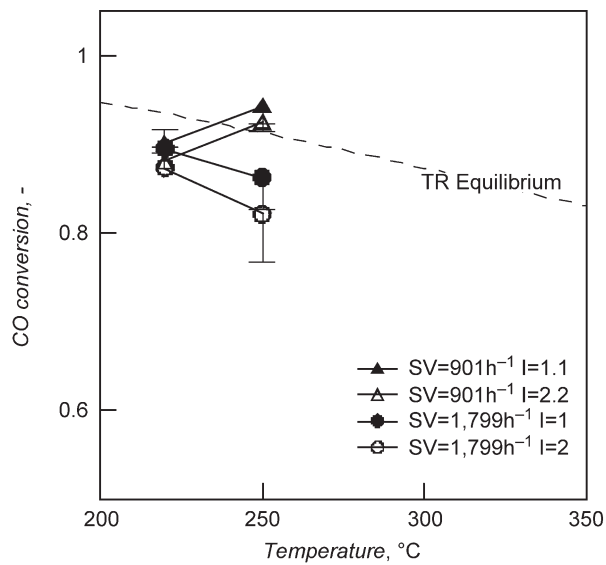


Figure 16: UniTwente 6—CO conversion vs. T . Average values (symbols) and mass balance on carbon (connected horizontal dash).

TABLE 7
UNIZARAGOZA MEMBRANES—PERMEATION EXPERIMENTS

Membrane	$T, ^\circ\text{C}$	Sweep, $\mu\text{mol/s}$	Permeance, $\text{nmol/m}^2 \text{ s Pa}$				idealSF - H_2/N_2
			H_2	N_2	CO_2	CH_4	
UniZaragoza 1	150	–	117	42	–	–	2.80
	200	–	125	42	42	67	3.00
UniZaragoza 2	255	16.6	113		56		
		51.4	124		59		
		52.1	154		100		

$p^{\text{Permeate}} = 101 \text{ kPa}$.

The UniZaragoza 1 was tested following the pressure drop method ($\Delta P^{\text{TM}} = 50 \text{ kPa}$), while for the UniZaragoza 2 the concentration gradient method was adopted, since Zaragoza University suggested maintaining $\Delta P^{\text{TM}} = 0$.

The experimental data for the UniZaragoza 1 showed that H_2 is the most permeable species and its permeance increases slightly with temperature. Also, for the UniZaragoza 2 H_2 was much permeable than CO_2 ; furthermore, the sweep gas increased the permeating fluxes.

MR Experiments Using UniZaragoza Membranes

Reaction experiments on the UniZaragoza 2 membrane were performed at 260, 288, 307, 338 $^\circ\text{C}$, varying the sweep factor (1–4); no ΔP^{TM} was employed. The catalyst weight was 1.02 g.

In Figure 17 the reaction data obtained at $\text{SV} = 1104 \text{ h}^{-1}$ are reported. The effect of an increase in the operating temperature is an increase in the CO conversion up to 307 $^\circ\text{C}$. A further increase in the reaction temperature up to 338 $^\circ\text{C}$ resulted in experimental points following the thermodynamic trend of the TR equilibrium. CO conversion higher than the TR-EC limit was obtained at 307–338 $^\circ\text{C}$, depending on the sweep factor. At the lowest sweep factor value ($I = 1$) CO conversion was below the TR equilibrium. Particularly, at $I = 2$, an increase in the operating temperature allowed significant improvements in CO conversion with respect to a TR. For $I = 3, 4$ better conversions, slightly above TR-EC, were obtained.

An increase in SV (1906 h^{-1}) results in a CO conversion lower than TR-EC (Figure 18). For an ideal membrane, an increase in CO conversion is predicted with the sweep factor increase. The beneficial effect of the sweep factor increase was observed also at 307 $^\circ\text{C}$, but only at the lowest SV considered (1104 h^{-1}). However, working at $\text{SV} = 1906 \text{ h}^{-1}$, a decreasing trend with the sweep factor was observed.

TR Experiments

WGS reaction tests were also carried out using a tubular TR in which the low temperature shift catalyst was packed. The reaction temperature was measured by means of a thermocouple inserted in the catalyst bed. These reaction experiments were performed at a high SV ($15,500 \text{ h}^{-1}$).

TR characteristics are: ID = 7 mm, reactor length = 50 mm, reactor volume = 1.92 cm^3 , catalyst weight = 1.9 g. The operating variables were the following: $T = 214\text{--}325 \text{ }^\circ\text{C}$, $\text{SV} = 1890\text{--}15,050 \text{ h}^{-1}$.

Reaction experimental data at $m = 0.98$ are reported in Figure 19. The data obtained at $\text{SV} = 2220 \text{ h}^{-1}$ showed an increasing CO conversion with T . In particular, a conversion value close to the TR-EC was obtained at 265 $^\circ\text{C}$. The same trend was observed for the data obtained at a high SV ($15,050 \text{ h}^{-1}$); therefore, kinetics was controlling at the two SV values.

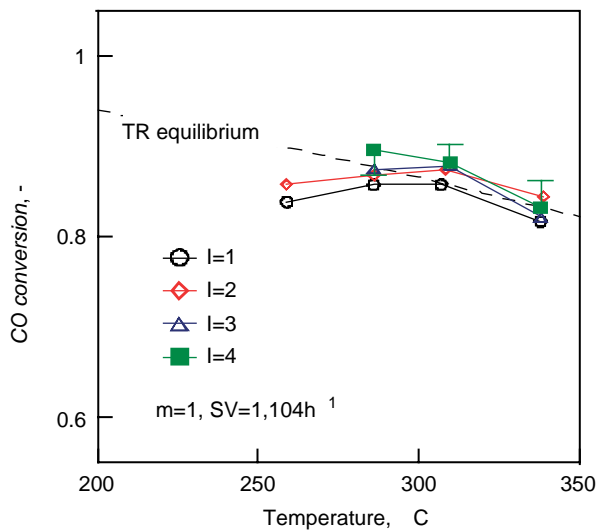


Figure 17: UniZaragoza 2—CO conversion vs. temperature at SV = 1104 h⁻¹.

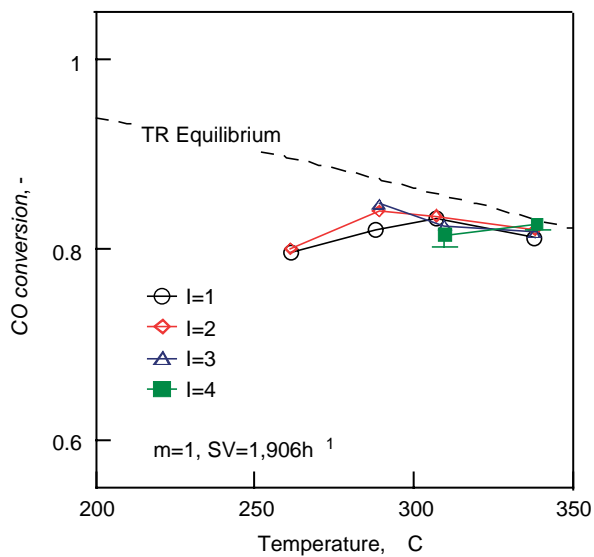


Figure 18: UniZaragoza 2—CO conversion vs. temperature at SV = 1906 h⁻¹.

However, the data obtained at a high SV (15,050 h⁻¹) showed a consistent reduction in CO conversion. The space velocity increase, in fact, determines a decrease in the residence time of the reagents on the catalytic bed; as a consequence, CO conversion is low and far from the equilibrium curve, even at temperatures up to 320 °C.

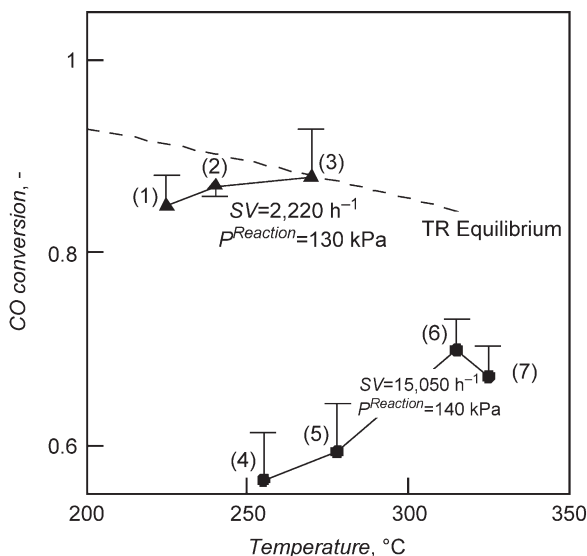


Figure 19: CO conversion vs. T in TR. Average values (symbols) and mass balance on carbon (connected horizontal dash).

CONCLUSIONS

The experimental work provided valuable information about the different membrane types (Pd/Ag supplied by SINTEF (Norway), silica by the University of Twente (The Netherlands) and Pd-based membranes by the University of Zaragoza (Spain)) and gave useful experimental information on the membrane WGS reactor concept.

The influence of different parameters on MR CO conversion, such as temperature, pressures, space velocity, sweep factor and partial pressure difference was investigated.

Initial tests were performed with a pure CO and H₂O mixture which is not a realistic feed to a WGS reactor and might lead to hot spots on the catalyst surface. Successive experiments involved either a traditional WGS reactor upstream of the MR or a synthesized gas mixture similar to the product gas from an oxygen-blown ATR (20% CO, 20% H₂O, 10% CO₂, 50% H₂), which gave a more realistic indication of the MR performance in an industrial application.

Temperature plays a very important role on the MR. The rate determining step, at a low temperature, is the kinetics; the membrane is not profitably utilized for the low H₂ concentration and even if the MR CO conversion is higher than that of a TR, it does not overcome the TR-EC. A high temperature and a low SV allow the thermodynamic limit of a TR to be overcome. Furthermore, increasing the ΔP^{TM} (up to 200 kPa), the CO conversion resulted above the TR-EC limit, also at high SV ($\sim 2000 \text{ h}^{-1}$), confirming the interest in MRs.

The CO conversion measured in MRs (using the membranes supplied by all the three partners) overcame the TR-EC limit, depending on the operating parameters: mainly temperature and space velocity. In particular, since WGS reaction has a low kinetic rate, better results were achieved working at a lower SV and higher temperatures ($> 250 \text{ }^\circ\text{C}$), e.g. 95% CO conversion was reached at $280 \text{ }^\circ\text{C}$.

The Pd-based tubular membranes supplied by SINTEF showed how the use of an MR, allowing H₂ separation, gives the possibility of overcoming the CO TR-EC at a temperature higher than $250 \text{ }^\circ\text{C}$. Better

results were achieved adopting a configuration that couples a TR and an MR: the rate determining step changed from kinetics (only MR) to thermodynamic one (TR + MR). As a consequence, higher CO conversion values were obtained working at the lowest experimental temperature. A complete CO conversion was reached using a TR + MR configuration at $SV_{MR} = 482 \text{ h}^{-1}$ and $I = 4.5$; however, an interesting CO conversion, well above the TR-EC limit, was achieved in the same configuration (TR + MR) at a higher $SV_{MR} = 1770 \text{ h}^{-1}$. Successive experiments, using an “ATR exit + Extra Steam” stream, allowed a significant improvement with respect to the TR-EC limit.

H_2 was the most permeable species in (tubular and flat) silica membranes supplied by the University of Twente. The reaction measurements were performed in a wide range of operating parameters (e.g. 210–320 °C, 100–550 kPa, 826–2,000 h^{-1}). CO conversion measured in MRs overcame the CO TR-EC at temperature ≥ 250 °C. The positive effect of the reaction pressure was also observed: with the UniTwente 1 membrane: by increasing the reaction pressure (up to 550 kPa) CO conversion was over the thermodynamic TR-EC at temperature higher than 250 °C.

Also, in Pd-based membranes supplied by the University of Zaragoza H_2 was the most permeable species. As suggested by the University of Zaragoza, no ΔP^{TM} was used during reaction tests (performed in the temperature range 260–338 °C) to avoid any membrane damage. However, also in this case, CO TR-EC was slightly overcome, depending on the operating conditions, particularly at low SV and high sweep factor. An increase in the operating temperature allowed improvements in CO conversion with respect to a TR up to 307 °C; at higher temperature no significant improvement was observed.

Reaction experiments were also performed on TR with SV values up to 15,050 h^{-1} . These data evidenced the negative effect of an SV increase on the CO conversion. A high SV determines a low residence time and, as a consequence, CO conversion is low and far from the equilibrium curve even at a high temperature.

NOMENCLATURE

MR	Membrane reactor
TR	Traditional reactor
TR-EC	TR equilibrium conversion, the maximum conversion achievable in a TR

List of Symbols

F	Molar flow rate [mol/s]
$I = \frac{F^{\text{Sweep}}}{F_{\text{CO}}^{\text{Feed}}}$	Sweep factor: ratio between flow rate of sweep gas and reference component [–]
J	Permeation flux [mol/m ² s]
m	Feed molar ratio H_2O/CO [–]
P	Pressure [Pa]
Permeance _i = $\frac{\text{Permeating Flux}_i}{\Delta P_i^{TM}}$	Permeance [mol/m ² s Pa]
Q	Volumetric flow rate [cm ³ (STP)/min]
actual $SF = \frac{(x_i/x_j)^{\text{Permeate}}}{(x_i/x_j)^{\text{Retentate}}}$	Separation factor, measured for gas mixture [–]
ideal $SF = \frac{\text{Permeance}_i}{\text{Permeance}_j}$	Separation factor, measured as pure gases [–]
$SV_{MR} = \frac{Q^{\text{Feed}}}{V_{\text{Catalyst}}}$	MR space velocity [h^{-1}]
$SV_{TR} = \frac{Q^{\text{Feed}}}{V_{\text{Catalyst}}}$	TR space velocity [h^{-1}]

T	Temperature [°C]
$\Delta P_i^{\text{TM}} = ((P^{\text{Feed}} + P^{\text{Retentate}})_i - (P^{\text{Sweep}} + P^{\text{Permeate}})_i)/2$	Trans-membrane difference of species partial pressure [Pa]
$\vartheta = \frac{F^{\text{Permeate}}}{F^{\text{Feed}}} = \frac{Q^{\text{Permeate}}}{Q^{\text{Feed}}}$	Stage-cut [-]
$\vartheta_i = \frac{F_i^{\text{Permeate}}}{F_i^{\text{Feed}}} = \frac{Q_i^{\text{Permeate}}}{Q_i^{\text{Feed}}}$	Stage-cut for the <i>i</i> th species [-]
<i>Superscript</i>	
Feed	Inlet stream on reaction side
Permeate	Outlet stream on permeation side
Retentate	Outlet stream on reaction side
Sweep	Inlet stream on permeation side

ACKNOWLEDGEMENTS

This work was developed within the framework of the GRACE project co-funded by the EU and the CCP (CO₂ Capture Project). The authors thank Dr. Rune Bredesen and Mr. Hallgeir Klette of SINTEF (Norway), Prof. Henk Kruidhof and Prof. Nieck Benes of the University of Twente (The Netherlands), Prof. Miguel Menendez and Dr. Maria Pilar Pina of the University of Zaragoza (Spain) for supplying the membrane. The authors also thank Haldor-Topsoe for supplying the catalyst.

REFERENCES

1. G. Barbieri, G. Marigliano, G. Perri, E. Drioli, Conversion-temperature diagram for a palladium membrane reactor. Analysis of an endothermic reaction: methane steam reforming, *Ind. Engng. Chem. Res.* **40** (2001) 2017–2026.
2. G. Marigliano, G. Barbieri, E. Drioli, Equilibrium conversion for a palladium membrane reactor. Dependence of the temperature and pressure, *Chem. Eng. Proc.* **42** (2003) 231–236.
3. E. Kikuchi, S. Uemiyama, N. Sato, H. Inoue, H. Ando, T. Matsuda, Membrane reactor using microporous glass-supported thin film of palladium. Application to the water gas shift reaction, *Chem. Lett.* (1989) 489–492.
4. A. Criscuoli, A. Basile, E. Drioli, An analysis of the performance of membrane reactors for the water-gas shift reaction using gas feed mixtures, *Cat. Today* **56** (2000) 53–64.
5. A. Basile, G. Chiappetta, S. Tosti, V. Violante, Experimental and simulation of both Pd and Pd/Ag for a water-gas shift membrane reactor, *Sep. Purif. Tech.* **25** (2001) 549–571.
6. G. Marigliano, G. Barbieri, E. Drioli, Effect of energy transport on a palladium-based membrane reactor for methane steam reforming process, *Cat. Today* **67/1–3** (2001) 87–101.
7. H. Imai, H. Morimoto, A. Tominaga, H. Hirashima, Structural changes in sol–gel derived SiO₂ and TiO₂ films by exposure to water vapour, *J. Sol–Gel Sci. Tech.* **10** (1997) 45–54.
8. S. Giessler, L. Jordan, J.C. Diniz da Costa, G.Q. Lu, Performance of hydrophobic and hydrophilic silica membrane reactors for the water gas shift reaction, *Sep. Purif. Tech.* **32** (2003) 255–264.